This research was originally published in: Mol Cancer Res. Jessie Zhong, Cuc T. Bach, Michael S.Y. Shum, Geraldine M. O'Neill, NEDD9 Regulates 3D Migratory Activity Independent of the Rac1 Morphology Switch in Glioma and Neuroblastom. (2014); 12(2); 264–73, DOI: 10.1158/1541-7786.MCR-13-0513

Final publication is available at:

http://mcr.aacrjournals.org/content/12/2/264.long

NEDD9 regulates glioma and neuroblastoma cell 3D migration independently of the Rac1-dependent morphology switch.

Jessie Zhong[1,2^], Cuc T Bach[1^], Michael S. Y. Shum[1] and Geraldine M. O'Neill[1,2*].

[1]Children's Cancer Research Unit, Kids Research Institute, The Children's Hospital at Westmead, NSW, Australia 2145, and [2]Discipline of Paediatrics and Child Health, The University of Sydney, NSW, Australia

^These authors contributed equally

*Corresponding Author:
Geraldine M. O'Neill
Children's Cancer Research Unit
Kids Research Institute
The Children's Hospital at Westmead
Locked Bag 4001, Westmead, 2145
Australia
Ph: 61 2 98451206
Fax: 61 2 98453078
Email: geraldine.oneill@health.nsw.gov.au

Running title: NEDD9 and 3D migration in glioma and neuroblastoma
Keywords: NEDD9, Rac GTPase, 3D migration, neuroblastoma, glioblastoma
Financial Support: This study was supported by National Health and Medical Research Council (NHMRC) grant 632515 (GO) and NSW Cancer Council grant RG12/06 (GO). JZ was supported by a post-graduate scholarship from the University of Sydney and a NSW Cancer Institute Scholar Award. CTB was supported by a C4-Fellowship from The Kids Cancer Project.
Conflict of interest. The authors declare no conflict of interest.
Word count: 4872 + 6 Figures

Abstract

Metastasizing tumour cells must transmigrate the dense extra-cellular matrix that surrounds most organs. The use of 3-dimensional (3D) collagen gels has revealed that many cancer cells can switch between different modes of invasion that are characterized by distinctive morphologies (rounded versus elongated). The adhesion protein NEDD9 can regulate the switch between elongated and rounded invasion in melanoma cells and thus we questioned the role of NEDD9 in the invasion switch of glioblastoma and neuroblastoma tumours that similarly derive from populations of neural crest cells. siRNA mediated depletion of NEDD9 failed to induce cell rounding in the glioma or neuroblastoma cells, contrasting the effects that have been described in melanoma and fibroblasts. Given that Rac GTPase has been described to mediate the switch between elongated and rounded invasion we tested whether the Rac morphology switch is functional in the glioma and neuroblastoma cells under investigation. Using both dominant negative Rac and Rac1-specific siRNA we confirm the presence of this morphological switch in the neuroblastoma, but not the glioma cells. In the absence of a morphological change following NEDD9 depletion we instead quantified cell migration speed and demonstrated a significant decrease in migration rate. Our data therefore reveal that NEDD9 can regulate 3D migration speed independently of the Rac1 morphology switch.

IMPLICATIONS: Our data suggests that targeting NEDD9 does not stimulate adaptive changes in glioma and neuroblastoma invasion and thus may be therapeutically useful for these tumours.

Introduction

The adhesion docking protein NEDD9/HEF1/Cas-L is a member of the Cas family of proteins that includes p130Cas/Bcar1, Efs/Sin and HEPL/CASS4.[1] Increasing studies point to a critical role for NEDD9 as a regulator of migration and invasion in diverse cancer types.[2] In addition to this pathological role, NEDD9 was first identified in a screen for neural precursor cell and developmentally down-regulated genes[3] and was subsequently shown to regulate migration in neural pre-cursor/neural crest cells.[4] The neural crest cells are a highly migratory cell type that give rise to a variety of cell lineages that includes peripheral neurons, glia and melanocytes.[5] In turn, transformation of neural crest cell populations is thought to give rise to neuroblastoma, glioma brain tumours and melanoma. Progression to invasive disease remains a significant impediment to successful treatment for each of these tumour types. The neuroblastomas are the most common extra-cranial tumour of childhood and the majority of patients present with metastatic disease. In contrast to other tumour types, gliomas rarely metastasize to secondary sites but instead the high grade gliomas (grade III and IV) extensively infiltrate the surrounding health brain tissue. Based on recent insights into the role of NEDD9 in the invasive behaviour of melanoma[6, 7] we have investigated the role of NEDD9 in glioma and neuroblastoma invasion that exhibits the features of invading neural crest cells.

NEDD9 is expressed during embryonic brain development but is down-regulated in the normal adult brain[3] upon lineage commitment of progenitor cells.[8] NEDD9 is specifically expressed in nestin-positive neural crest cells that emigrate from the dorsal tube.[4] The characteristic invasive morphology of the neural crest cells is

suggested to closely resemble that of invasive glioma cells. [9, 10] Uniquely among the Cas family proteins, NEDD9 was required for the invasion of U87MG glioblastoma cells through brain homogenates.[11] NEDD9 is elevated in high grade glioma cells and high level expression in low grade glioma correlated with significantly poorer prognosis and increased invasion.[12] In contrast, the morphological regulation of invasive neuroblastoma is comparatively less well defined. Notably, NEDD9 was defined as an all trans-retinoic acid responsive gene upregulated in response to retinoic acid induced neuritogenesis in neuroblastoma cells.[13]

3D collagen gels that mimic the *in vivo* interstitial environment have been key in demonstrating the plasticity of cancer cell invasion mechanisms.[7, 14, 15] It has emerged that cancer cells may employ differential modes of invasion characterised by distinct cellular morphologies. In particular NEDD9 promotes elongated/mesenchymal invasion in melanoma cells.[7] Elongated invasion is regulated by Rac GTPase activity and Rac GTPase inhibition stimulates the switch to a rounded/amoeboid, Rho kinase-dependent mode of invasion. NEDD9 stimulates Rac GTPase activity via the recruitment of the Rac GTP exchange factor DOCK3.[7] Depletion of NEDD9 from melanoma cells[7] and mouse embryo fibroblasts[16] leads to a switch from an elongated phenotype to a rounded cell phenotype in 3D collagen cultures.

A number of studies have identified a key role for Rac activity in regulating high grade glioma invasion. While Rac1 depletion reduced glioma cell line invasion[17], this treatment alone was insufficient to induce a switch to a rounded invasion mode.[15] It was only following inhibition of all Rac activity via knock-down of both Rac1 and

Rac3 isoforms or expression of dominant negative Rac that U87MG cells adopted the classic rounded invasion mode.[15] Similarly, simultaneous Rac1 and Rac3 depletion, together with Rho kinase inhibition, was required in order to comprehensively arrest 3D collagen invasion by highly invasive cells isolated from the peri-tumoral region of a high grade glioma.[18] While there appears to be no reports to date having examined whether neuroblastoma cells undergo morphological transition in 3D collagen culture following Rac inhibition, in 2D conditions Rac1 and Rac3 isoforms have apparently opposite effects on cellular morphologies.[19] These studies therefore suggest that Rac GTPase may be a critical determinant of high grade glioma and neuroblastoma 3D morphologies.

In the present study we have investigated the role of NEDD9 in regulating 3D invasive morphologies of high grade glioma and neuroblastoma cells. Using publicly available expression data we show a significant association between NEDD9 expression and poor survival rates for both tumour types. Importantly, in contrast to effects seen in melanoma, NEDD9 depletion fails to induce a morphological switch in either high grade glioma or neuroblastoma cells. Notably, while the neuroblastoma cells exhibit a robust morphological switch in response to Rac inhibition, this affect is much reduced in the high grade glioma cells. Instead, we find that NEDD9 depletion significantly reduces migration speed of cells as they negotiate the 3D collagen environment. Collectively, our data reveal that NEDD9 plays a significant role in regulating cell speed in 3D environments, independently of the Rac-mediated morphological switch.

Materials and Methods

Cell culture and antibodies. Cultured glioblastoma (A172, CCF-STTG1, DBTRG, MO59J, MO59K and T98G) cell lines were kindly provided by Dr Kerrie McDonald (Lowy Cancer Centre, UNSW, Australia). Correct identity of A172 and DBTRG lines was independently verified by CellBank Australia (Sydney, Australia). The neuroblastoma cell lines (NB69, SH-EP, SH-SY5Y, SK-N-AS, SK-N-FI and SK-N-SH) were kindly provide by Dr Loretta Lau (Kids Research Institute, Sydney, Australia). Cell lines were maintained in DMEM supplemented with 10% FBS. Growth of cells in 3D collagen gels, media for live imaging and invasion assays through 3D collagen gels was based on protocols previously reported to identify invasion plasticity[20] and as we have previously employed [21]. The following antibodies were used: anti-NEDD9 (ImmuQuest; clone 2G9 and Cell Signaling Technology, clone 29G); Anti-pan-Rac (#610650 BD Bioscience), anti-HSP70 and anti-α-tubulin (Sigma-Aldrich); HRP-conjugated anti-mouse and anti-rabbit (Amersham and Biorad) and anti-rat Alexa-Fluor 647 conjugate (Molecular Probes, Invitrogen).

Protein extraction, siRNA and immunoblotting. Conditions of protein extraction and immunoblotting were carried out as previously described.[22] Protein concentrations were determined using the BCA Protein Assay Kit (Pierce Biotechnology IL, USA) and protein concentrations equalized prior to loading on gels. Control siRNA and custom-designed NEDD9 siRNAa (targeting the sequence CCAGGACAUUCGCAACAAA, as previously described[16]) and siRNAb (GAGACACCAUCUACCAAGUUU, as previously described[7]) were purchased from Dharmacon (Thermo Scientific). 10 nM siRNA was transiently transfected twice at 24 h intervals, using Lipofectamine2000 (Life Technologies) as per manufacturer's

instructions. Inhibition of Rac GTPase activity was achieved by transfecting cells with plasmid vector encoding dominant negative Rac (DNRac) as previously described.[23] Custom designed Rac siRNAs were purchased from Invitrogen comprising sequences targeting human Rac1 (5'-GAGGCCUCAAGACAGUGUUUGACGA-3') and Rac3 (5'-CCUCCGCGACGACAAGGACACCAUU-3'); control sequences for Rac knockdown experiments were Qiagen Allstar Non-targeting Control siRNA (Qiagen). Rac siRNAs were used at a final concentration of 100nM when used individually and 50nM each when used in combination. Successful knock-down was independently confirmed for all experiments.

Live cell imaging, migration and rounding analysis. Time-lapse images were captured using an ORCA ERG cooled CCD camera (Hamamatsu, SDR Clinical Technology NSW, Australia) and Olympus IX81 inverted microscope equipped with an environmental chamber heated to 37^0C. Transmitted light images were captured at indicated time intervals. Cells undergoing division or apoptosis were excluded from analyses and random migration analyses were performed on sparsely plated cultures. Post image capture, nuclear translocation was tracked in time-lapse stacks using Metamorph V6.3 software (Molecular Devices). Calculation of Mean Squared Displacement (MSD) was performed as previously described.[24] We note that only elongated cells were tracked in the analysis of 3D migration. Glioblastoma cell morphologies in 3D collagen gels were manually scored as either elongated, displaying extending protrusions and an elongated cell body, or rounded, with a rounded cell body and the absence of protrusions. Cells were counterstained with propidium iodide (Sigma-Aldrich) and apoptotic cells excluded from morphological analyses. Reduced cell branching exhibited by the SH-EP cells facilitated semi-

automated analysis of cell shapes. In this case z-stacks of fluorescently-tagged phalloidin stained cells were captured using Leica SP5 confocal scanning laser microscope (Leica Microsystems, Germany) with 10X air objective. Maximum projections of z-stacks were filtered using Metamorph V7.7 software by Fast Fourier Transformation followed by low pass basic filter, auto-thresholding for light objects and drawing regions around objects. Any joined cells were manually separated and cell shape factor ($4\pi A/P^2$: A = area, P = perimeter) then measured using integrated morphology analysis. Data were filtered to exclude anything smaller than 15 pixels in area. Cells with shape factor >0.75 were scored as rounded.

Image preparation. Final micrograph images and grey level adjustments were prepared in Adobe Photoshop.

RESULTS

NEDD9 expression in glioma and neuroblastoma

We first examined the relationship between NEDD9 expression and patient survival in both glioma and neuroblastoma. This was achieved using publicly available data from the REpository for Molecular BRAin Neoplasia DaTa (REMBRANDT) homepage (http://rembrandt.nci.nih.gov) and the Oncogenomics website (http://home.ccr.cancer.gov/oncology/oncogenomics/) for neuroblastoma. In agreement with previously published results[12], high level NEDD9 expression was significantly associated with poorer survival rates in a cohort of glioma patients (Figure 1A). Moreover, comparison of the percentage of low grade gliomas (grade II/III) and high grade gliomas (grade IV, glioblastoma) between cases with intermediate versus high level NEDD9 expression revealed significantly more high grade glioma cases in the high NEDD9 dataset (Figure 1B). Notably, we found a significant association between high NEDD9 expression and reduced patient survival in the subset of neuroblastomas that lack N-myc amplification (n = 101) (Figure 1C). Based on these observations, NEDD9 expression was then profiled in human glioblastoma cell lines, and neuroblastoma lines that lack N-myc amplification. The highest level of NEDD9 expression (seen as a doublet on western blot[25]) was detected in the A172, DBTRG and MO59J glioblastoma cells and in the SH-EP and SK-N-SH neuroblastoma cells (Figure 1D). The SK-N-SH cells are a mixed culture from which both the SH-EP and SH-SY-5Y cell lines were derived.[26] It is therefore interesting that while the SH-EP and SK-N-SH lines are positive for NEDD9 the SH-SY-5Y cells exhibit little detectable NEDD9, suggesting that SK-N-SH cells may be a mix of high and low NEDD9 expressing cells.

NEDD9 depletion does not induce rounding

It has previously been established that NEDD9 regulates the morphological switch from elongated to rounded 3D invasion in melanoma cells.[7] Thus we questioned the effect of NEDD9 depletion on glioblastoma cell morphology, focusing on the A172 and DBTRG cells due to their high endogenous levels of NEDD9 expression. Under 3D culture conditions, ~60% of the A172 cells and ~40% of DBTRG cells have an elongated morphology (Figure 2B and 2C). Inspection of cells following NEDD9 depletion suggested little evidence of a switch to a rounded morphology in either cell line, despite robust NEDD9 depletion (Figure 2A and 2B). Rather, quantification indicated that NEDD9 depletion caused a small decrease in the percentage of round A172 and DBTRG cells (Figure 2C). Thus, NEDD9 depletion does not appear to induce rounding in either A172 or DBTRG glioblastoma cells.

We next questioned the effect of NEDD9 depletion on neuroblastoma cell morphology, using the SH-EP line that has high endogenous NEDD9 expression (Figure 1C). In 3D collagen gels, the SH-EP cells have a mixed morphology with ~ 50% of cells exhibiting an elongated phenotype (Figure 2D and 2F). NEDD9 depletion was achieved using two independent siRNA sequences (siRNAa and siRNAb) (Figure 2E). Again, visual inspection of the cultures suggested little effect on cell rounding (Figure 2D). Quantification revealed that NEDD9 depletion with siRNAa caused a small decrease in the percentage of round cells, while siRNAb caused a small increase in cell rounding (Figure 2F). However this only represented a change from an average of 53% rounded under control conditions, to 50% and 57%, respectively. Thus, in contrast to effects on melanoma cells[7] and fibroblasts[16] the

present data suggest that NEDD9 depletion has a minimal effect on the morphology of either glioblastoma or neuroblastoma cells.

Differential response to Rac1 inhibition

We considered that the lack of effect of NEDD9 depletion on the cell morphologies may reflect absence of the morphological switch (elongated/mesenchymal to rounded/amoeboid) in these cells. Rac GTPase is a major regulator of the switch between elongated and rounded invasion[7, 15] and NEDD9 is an upstream regulator of this pathway in melanoma cells.[7] Thus we tested whether inhibition of Rac GTPase activity via the expression of dominant negative Rac (GFP.DNRac) induced morphological transition in either the A172 or SH-EP cells. Dominant negative Rac resulted in only a modest increase in the numbers of rounded A172 glioblastoma cells (Figure 3A). By contrast, approximately 80% of SH-EP cells expressing GFP.DNRac exhibited a rounded phenotype (Figure 3A). This is highlighted in 10 random fields of view for GFP versus GFP.DNRac transfected SH-EP cells where the GFP-positive control cells display a mix of elongated and rounded morphologies, while all visible GFP.DNRac-positive cells are rounded (Figure 3B). These data suggest that while the Rac-dependent morphology switch is strongly present in the SH-EP cells, loss of Rac activity appears to have less effect in the A172 cells.

Previous studies targeting Rac isoforms revealed that switching U87MG glioblastoma cells from an elongated to a rounded morphology requires the depletion of both Rac1 and Rac3 isoforms[15]. This suggested the possibility that the failure to induce rounding in A172 cells following NEDD9 depletion may be due to NEDD9 regulating a specific isoform of Rac and that the presence of other Rac isoforms may therefore

compensate. Rac 3 is highly expressed in the brain[27] and both Rac1 and Rac3 are suggested to play a key role in glioblastoma invasion.[28] Thus we questioned whether A172 rounding may require the inhibition of both Rac1 and Rac3 isoforms. Depletion was achieved using siRNA-specific for each Rac isoform as previously described.[15] Due to the absence of commercially-available isoform specific antibodies, confirmation of knock-down was determined by comparing the levels of total Rac protein (Figure 4A). Notably, only siRNA targeting Rac1, not Rac3, significantly decreased levels of total Rac protein (Figure 4B). Since it has previously been suggested that Rac3 depletion may lead to a corresponding increase in Rac1 protein[15], we proceeded with the double knock-down of Rac1 and Rac3 and examined the morphology of cells resulting from all three siRNA conditions. This analysis revealed that combined depletion of Rac1 and Rac3 had no effect on cellular morphologies in 3D collagen gels (Figure 4C and 4D). Similarly, individual targeting of the Rac isoforms had no effect on A172 morphology. It is interesting that Rac knock-down was not able to recapitulate the small increase in rounding that was seen in cells expressing dominant negative Rac (Figure 3), despite a significant reduction in total Rac protein levels (Figure 4A). Together, these data emphasize that the A172 cells have a limited response to the Rac-dependent morphology switch.

Given that the Rac morphology switch appears to be robustly functioning in the SH-EP cells, we next questioned the isform-specific role of Rac in SH-EP 3D morphology. While Rac1 depletion significantly reduced total Rac protein levels, Rac3 depletion had no effect (Figure 5A and 5B) either that Rac3 may not be expressed in the SH-EP cells, or there is a compensating increase in Rac1 as suggested earlier. Critically, Rac1 depletion significantly increased the numbers of

rounded SH-EP cells (Figure 5C and D), mimicking the effect of DNRac. In summary, these data suggest that the morphological switch in SH-EP cells is Rac1 dependent.

NEDD9 depletion slows 3D migration.

Our investigations have revealed distinct differences in the morphological control of A172 glioblastoma and SH-EP cells in 3D collagen gels, despite both lines expressing high levels of endogenous NEDD9 protein. Moreover, the data suggest that NEDD9 does not regulate a Rac1-dependent molecular switch in these cell lines. This then raises the question of whether NEDD9 plays any role in the 3D migration of these cells. To examine this question we measured 3D migration speed by analysis of time-lapse images of the cells as they migrate through the 3D collagen gels. This revealed that the A172 cells move more slowly through the gels following NEDD9 depletion. Reduced NEDD9 levels caused a shift in the Mean Squared Displacement (MSD) and a significant decrease in average cell speed (Figure 6A and 6B). Similarly, the DBTRG cells (that also do not undergo rounding following NEDD9 depletion, as demonstrated in Figure 2) slow down following NEDD9 depletion (Figure 6A and 6B). Finally, we also observed that the SH-EP cells slow down in response to treatment with either siRNAa or siRNAb targeting NEDD9. When tracking the SH-EP cells following NEDD9-depletion there appeared to be two populations of cells. One fast moving group appeared to be relatively unaffected by NEDD9 depletion. However, the slower moving group was more affected. Comparison of the frequency distrition of speeds between the different conditions revealed that the greatest changes occurred at speeds $\leq$ 0.4 μm/min (Figure 6C). Accordingly, the average speed was significantly lower in the <0.4 μm/min populations treated with either NEDD9-

targeting siRNA (Figure 6D). Notably, following NEDD9 knock-down the cells continued to display rounded cell bodies with a leading membrane protrusion, with occasional pausing as the cells retracted the protrusion and adopted a rounded shape, but had slower progress through the gel (Figure 6E). Together these data reveal that NEDD9 depletion reduces 3D migration speed, without stimulating transition to rounded invasion.

Discussion

Based on insights from developmental biology, in the present study we have investigated the role for NEDD9 in the migration of tumours that derive from neural crest cell populations. We employed 3D collagen gel models to investigate invasion plasticity in response to altered NEDD9 expression.[7, 20] Importantly, while we show cell-type differences in regard to invasion plasticity control by Rac GTPase activity, the cell lines investigated in the present study are united by their lack of morphological switch following NEDD9 depletion. Thus our data suggest that NEDD9 may not universally regulate the transition between morphologically distinct invasion phenotypes. Instead, we find that NEDD9 is an important determinant of the speed with which cells negotiate the 3D extracellular environment.

Prior to initiating investigations of NEDD9 and migration in glioma and neuroblastoma cell lines, we first determined whether there is any clinical association between NEDD9 and survival in these tumour types. Related to this, a recent study showed that higher level NEDD9 in lower grade glioma tumours is associated with reduced progression free survival.[12] In agreement with this, analysis of REMBRANDT data presented here demonstrated an association between NEDD9

expression and survival when all glioma tumours were grouped together. When NEDD9 levels were examined specifically in the high grade gliomas (III and IV) there was no significant association between expression and survival (data not shown). Importantly, recent advances in tumour profiling have revealed that high grade gliomas can be further stratified into risk groups based on gene expression profiles. For example, one such classification scheme defines cells as pro-neural, proliferative and mesenchymal, with corresponding increase in aggressiveness.[29] Potentially, NEDD9 expression may prove to be more prominent in one of these sub-classes, particularly given recent reports suggesting a correlation between NEDD9 and nestin expression in glioma.[12] We observed a striking inverse relationship between NEDD9 expression and patient survival in the sub-set of neuroblastomas that lack N-myc amplification. Critically, ~65% of patients with metastatic disease have no N-myc amplication and variable clinical behaviours of these tumours complicate treatment decisions thus there is an important need for molecular markers that can stratify these tumours.[30] Together, these analyses expand the range of tumour types in which high level NEDD9 expression has been correlated with reduced patient survival rates including melanoma[6], lung adenocarcinoma[31-33] and head and neck cancer.[34]

The biophysical constraints supplied by the 3D collagen gel model allow interrogation of invasion plasticity as cells adopt discrete morphologies (rounded versus elongated) reflective of the underlying invasion machinery. Using this approach we have shown that NEDD9 depletion failed to induce a switch in cellular morphologies in any of the cell lines under investigation. Notably, siRNAb targeting NEDD9 is identical to the sequence previously successfully used to induce a switch to rounded invasion in melanoma cells (equivalent to NEDD9 OT-4 targeting sequence[7]). Thus it appears

that there may be cell-type specific differences in the effects of NEDD9 on invasion plasticity. Importantly, we confirmed that the SH-EP cells exhibit a robust switch to rounded morphology following Rac1 depletion. Thus these cells are clearly competent to undergo morphological transition. By contrast, the A172 glioblastoma cells exhibited limited morphological transition following Rac inhibition. The small morphological change in A172 seen following dominant negative Rac inhibition is likely due to the well-described non-specific inhibition of other Rho family GTPases following high level expression of this construct[35].

In contrast to our data, other high grade glioma cell lines such as the U87MG cells undergo morphological transition to rounded invasion following Rac inhibition.[15] Both the A172 and DBTRG cell lines are positive for nestin and DLL3 (data not shown), markers that are associated with the pro-neural phenotype. Potentially, the ability of cells to switch between invasion modes (and use different routes of invasion throughout the brain) may also prove to track with sub-categories of high grade glioma. In contrast to the A172 cells, the SH-EP cells undergo morphological transition following Rac1 inhibition, but this is not phenocopied by NEDD9 inhibition. Similarly, we have previously shown that adoption of an arborized phenotype with neuritic membrane extensions is induced by combined NEDD9 and Rho kinase inhibition and cannot be blocked by Rac inhibition.[23] Thus, at least in these two examples it appears that NEDD9 may not be regulating cellular morphologies via activation of Rac1 GTPase.

The striking finding from our study is that in each case NEDD9 depletion significantly reduced the speed of 3D cell migration. Importantly, this suggests a

similar mechanism of NEDD9 action in these tumour types from diverse backgrounds. The 3D collagen matrix requires cells to either deform themselves in order to squeeze through pores in the matrix (rounded invasion) or alternatively deform the matrix via exerting force through adhesion to the matrix and secreting enzymes to degrade the matrix (elongated invasion).[36] Significantly, NEDD9 depletion reduced speed, without altering elongated morphologies. Similarly, *let-7i* microRNA-mediated inhibition of the Twist/NEDD9/Rac1 signalling pathway in head and neck cancer cells reduced the speed of elongated cell migration.[34] We have previously shown that mouse embryo fibroblasts lacking NEDD9 expression exhibited reduced adhesive force to the extra-cellular matrix.[16] Thus it is possible that the reduced migration speed exhibited following NEDD9 depletion may be due to decreased adhesive force to the surrounding matrix. Alternatively, given that NEDD9 has previously been shown to modulate matrix metalloproteinase expression[37], NEDD9 depletion may reduce matrix reorganization. Collectively, the common effect of NEDD9 on 3D cell speed suggests that targeting NEDD9 may be a useful therapeutic target in subsets of glioma and neuroblastoma tumour cells with high NEDD9 expression.

Legends

Figure 1. NEDD9 association with survival in glioma and neuroblastoma. Kaplan-Meier plots comparing patient survival according to NEDD9 expression are shown. A. The glioma cohort was dichotomised at 2 x the median NEDD9 expression value. A significant difference (p = 0.01, Logrank test) was observed between high level (red, n = 207) and intermediate level (blue, n = 135) NEDD9 expression with survival. Analysis was performed on data from the REpository for Molecular BRAin Neoplasia DaTa (REMBRANDT) homepage (http://rembrandt.nci.nih.gov), National Cancer Institute, accessed 2013, October 21. B. NEDD9 expression versus tumour grade. Percentages of grade II/III gliomas are shown in white and grade IV (glioblastoma) are shaded grey. Significant differences between the proportions of cases with high level NEDD9 expression are indicated (Fisher's Exact Test). C. Analysis of NEDD9 expression in non N-myc amplified neuroblastoma tumours[30] at the Oncogenomics website (http://home.ccr.cancer.gov/oncology/oncogenomics/). These cases are all from high risk patients with metastatic disease. The cohort was dichotomised at 2 x the average NEDD9 expression value. A significant difference (p = 0.0008, Logrank test) was observed between high level (red, n = 51) and low (blue, n = 50) NEDD9 expression with survival. D. NEDD9 expression detected by western blot in 6 glioblastoma cell lines and 6 non-N-myc amplified neuroblastoma cell lines. NEDD9 is detected as a doublet, corresponding to 105 kDa and 115 kDa phospho-forms. HSP70 or tubulin expression is shown as a loading control.

Figure 2. NEDD9 depletion does not cause cell rounding.

A. Western blot analysis with anti-NEDD9 antibodies showing depletion of NEDD9 protein in A172 and DBTRG cells following NEDD9-targeted siRNA. Blots were

probed with anti-HSP70 antibodies to demonstrate equal loading. B. A172 and DBTRG cell morphology in 3D collagen gels showing examples of elongated cells (arrow heads) and rounded cells (arrows). C. Histogram shows the percentage of rounded cells under the indicated conditions. Cells were counterstained with propidium iodide and apoptotic cells excluded from morphological analyses. Data averaged from >20 fields of view with 4 x objective. ** $p < 0.01$, Students' *t*-test. D. Morphology of SH-EP cells in 3D collagen gels under the indicated treatment conditions. Micrographs show maximum projections of confocal slices of the entire gel containing cells fixed and stained with fluorescently-tagged phalloidin. E. Western blot analysis with anti-NEDD9 antibodies showing depletion of NEDD9 protein in SH-EP cells following NEDD9 targeting with two independent siRNAs (a and b). Blots were probed with anti-HSP70 antibodies to demonstrate equal loading. F. Histogram shows the average numbers of rounded cells under each condition. Data represent the average from 3 fields of view, >250 cells per field. * $p < 0.05$, Students' *t*-test.

Figure 3. DN Rac induces cell rounding. A. Histogram showing the percentages of cells (A172 and SH-EP, as indicated) transfected with GFP control vector or GFP fused to dominant negative (DN) Rac displaying a rounded phenotype. Data represent the average from triplicate repeats, >60 cells scored per condition, per experiment. * $p < 0.05$, ** $p < 0.01$, Students' *t*-test. B. Bright field images of SH-EP cells in collagen overlayed with GFP fluorescence (10 examples shown per condition). Top panels show cells transfected with GFP empty vector and bottom panels with GFP.DNRac. Scale bar = 50 μm.

Figure 4. Rac1 depletion does not induce A172 rounding. A. Western blot showing total Rac protein levels in A172 cells following treatment with Rac1, Rac3 or combined Rac1/Rac3 siRNA. GAPDH levels are shown to confirm equal loading. B. Densitometry of total Rac protein levels following siRNA treatments as indicated. Data shown are the average fold change relative to controls from triplicate biological repeats. * $p < 0.05$, ** $p < 0.01$, *** $p < 0.001$, Students' *t*-test. C. Micrographs showing maximum projections of confocal slices of collagen gels containing cells, fixed and stained with fluorescently-tagged phalloidin and treated as indicated. D. Percentage of round cells in 3D collagen gels, treated as indicated. NS = not significant, Students' *t*-test.

Figure 5. Rac1 depletion induces SH-EP cell rounding. A. Western blot showing total Rac protein levels in SH-EP cells following treatment with Rac1, Rac3 or combined Rac1/Rac3 siRNA. GAPDH levels are shown to confirm equal loading. B. Densitometry of total Rac protein levels following siRNA treatments as indicated. Data shown are the average fold change relative to controls from triplicate biological repeats. *** $p < 0.001$, NS = not significant, Students' *t*-test. C. Micrographs showing maximum projections of confocal slices of collagen gels containing cells, fixed and stained with fluorescently-tagged phalloidin and treated as indicated. D. Percentage of round cells in 3D collagen gels, treated as indicated. * $p < 0.05$, NS = not significant, Students' *t*-test.

Figure 6. NEDD9 depletion reduces 3D migration speed. A. MSD calculated from trajectories of control (black squares) and NEDD9 siRNA-treated cells (white squares) in the indicated cell lines, migrating in 3D collagen gels. Data represent the

average of 3 (A172) and 5 (DBTRG) independent experiments (~50 cells tracked per experiment). B. 3D cell speed is significantly reduced following NEDD9 siRNA. ** $p < 0.001$, *** $p < 0.0001$, Students' *t*-test. C. Frequency distribution of SH-EP cell speeds following NEDD9 depletion as indicated. D. Comparison of the average SH-EP cell migration speeds <0.4 μm/min. ** $p < 0.001$, *** $p < 0.0001$, Students' *t*-test. E. Representative images from time-lapse series of SH-EP neuroblastoma cells in 3D collagen gels, showing characteristic morphologies under control conditions and following NEDD9 siRNA. Frames shown are from 0.5 hourly time intervals as indicated. Arrow heads point to the cell of interest. Scale bar, 20μm.

References

1. Singh M, Cowell L, Seo S, O'Neill G, Golemis E. Molecular basis for HEF1/NEDD9/Cas-L action as a multifunctional co-ordinator of invasion, apoptosis and cell cycle. Cell Biochem.Biophys 2007; 48: 54-72

2. O'Neill GM, Seo S, Serebriiskii IG, Lessin SR, Golemis EA. A New Central Scaffold for Metastasis: Parsing HEF1/Cas-L/NEDD9. Cancer Res 2007; 67: 8975-8979

3. Kumar S, Tomooka Y, Noda M. Identification of a set of genes with developmentally down-regulated expression in the mouse brain. Biochem Biophys Res Commun 1992; 185: 1155-1161

4. Aquino JB, Lallemend F, Marmigere F, Adameyko, II, Golemis EA, Ernfors P. The retinoic acid inducible Cas-family signaling protein Nedd9 regulates neural crest cell migration by modulating adhesion and actin dynamics. Neuroscience 2009; 162: 1106-19

5. Huang X, Saint-Jeannet JP. Induction of the neural crest and the opportunities of life on the edge. Dev Biol 2004; 275: 1-11

6. Kim M, Gans JD, Nogueira C, Wang A, Paik JH, Feng B et al. Comparative oncogenomics identifies NEDD9 as a melanoma metastasis gene. Cell 2006; 125: 1269-1281

7. Sanz-Moreno V, Gadea G, Ahn J, Paterson H, Marra P, Pinner S et al. Rac activation and inactivation control plasticity of tumor cell movement. Cell 2008; 135: 510-523

8. Aquino JB, Marmigere F, Lallemend F, Lundgren TK, Villar MJ, Wegner M et al. Differential expression and dynamic changes of murine NEDD9 in progenitor cells of diverse tissues. Gene Expr Patterns 2008; 8: 217-26

9. Kakita A, Goldman JE. Patterns and dynamics of SVZ cell migration in the postnatal forebrain: monitoring living progenitors in slice preparations. Neuron 1999; 23: 461-472

10. Beadle C, Assanah MC, Monzo P, Vallee R, Rosenfeld SS, Canoll P. The role of myosin II in glioma invasion of the brain. Mol Biol Cell 2008; 19: 3357-3368

11. Natarajan M, Stewart JE, Golemis EA, Pugacheva EN, Alexandropoulos K, Cox BD et al. HEF1 is a necessary and specific downstream effector of FAK that promotes the migration of glioblastoma cells. Oncogene 2006; 25: 1721-1732

12. Speranza MC, Frattini V, Pisati F, Kapetis D, Porrati P, Eoli M et al. NEDD9, a novel target of miR-145, increases the invasiveness of glioblastoma. Oncotarget 2012; 3: 723-34

13. Merrill RA, See AW, Wertheim ML, Clagett-Dame M. Crk-associated substrate (Cas) family member, NEDD9, is regulated in human neuroblastoma cells and in the embryonic hindbrain by all-trans retinoic acid. Dev Dyn 2004; 231: 564-575

14. Friedl P. Prespecification and plasticity: shifting mechanisms of cell migration. Curr Opin Cell Biol 2004; 16: 14-23

15. Yamazaki D, Kurisu S, Takenawa T. Involvement of Rac and Rho signaling in cancer cell motility in 3D substrates. Oncogene 2009; 28: 1570-1583

16. Zhong J, Baquiran JB, Bonakdar N, Lees J, Ching YW, Pugacheva E et al. NEDD9 stabilizes focal adhesions, increases binding to the extra-cellular matrix and differentially effects 2D versus 3D cell migration. PloS one 2012; 7: e35058

17. Chuang YY, Tran NL, Rusk N, Nakada M, Berens ME, Symons M. Role of synaptojanin 2 in glioma cell migration and invasion. Cancer Res 2004; 64: 8271-5

18. Ruiz-Ontanon P, Orgaz JL, Aldaz B, Elosegui-Artola A, Martino J, Berciano MT et al. Cellular plasticity confers migratory and invasive advantages to a population of glioblastoma-initiating cells that infiltrate peritumoral tissue. Stem Cells 2013; 31: 1075-85

19. Hajdo-Milasinovic A, Ellenbroek SI, van Es S, van der Vaart B, Collard JG. Rac1 and Rac3 have opposing functions in cell adhesion and differentiation of neuronal cells. J Cell Sci 2007; 120: 555-66

20. Wolf K, Mazo I, Leung H, Engelke K, von Andrian UH, Deryugina EI et al. Compensation mechanism in tumor cell migration: mesenchymal-amoeboid transition after blocking of pericellular proteolysis. J Cell Biol 2003; 160: 267-277

21. Lees JG, Bach CTT, Bradbury P, Paul A, Gunning PW, O'Neill GM. The actin-associating protein Tm5NM1 blocks mesenchymal motility without transition to amoeboid motility. Oncogene 2011; 30: 1241-1251

22. Cowell LN, Graham JD, Bouton AH, Clarke CL, O'Neill GM. Tamoxifen treatment promotes phosphorylation of the adhesion molecules, p130Cas/BCAR1, FAK and Src, via an adhesion-dependent pathway. Oncogene 2006; 25: 7597-7607

23. Bargon SD, Gunning PW, O'Neill GM. The Cas family docking protein, HEF1, promotes the formation of neurite-like membrane extensions. Biochim Biophys Acta 2005; 1746: 143-154

24. Mierke CT, Kollmannsberger P, Zitterbart DP, Smith J, Fabry B, Goldmann WH. Mechano-coupling and regulation of contractility by the vinculin tail domain. Biophys J 2008; 94: 661-670

25. Bradshaw LN, Zhong J, Bradbury P, Mahmassani M, Smith JL, Ammit AJ et al. Estradiol stabilizes the 105-kDa phospho-form of the adhesion docking protein NEDD9 and suppresses NEDD9-dependent cell spreading in breast cancer cells. BBA – Mol Cell Res 2011; 1813: 340-345

26. Biedler JL, Helson L, Spengler BA. Morphology and growth, tumorigenicity, and cytogenetics of human neuroblastoma cells in continuous culture. Cancer Res 1973; 33: 2643-2652

27. Wennerberg K, Rossman KL, Der CJ. The Ras superfamily at a glance. J Cell Sci 2005; 118: 843-6

28. Chan AY, Coniglio SJ, Chuang YY, Michaelson D, Knaus UG, Philips MR et al. Roles of the Rac1 and Rac3 GTPases in human tumor cell invasion. Oncogene 2005; 24: 7821-9

29. Phillips HS, Kharbanda S, Chen R, Forrest WF, Soriano RH, Wu TD et al. Molecular subclasses of high-grade glioma predict prognosis, delineate a pattern of disease progression, and resemble stages in neurogenesis. Cancer Cell 2006; 9: 157-73

30. Asgharzadeh S, Pique-Regi R, Sposto R, Wang H, Yang Y, Shimada H et al. Prognostic significance of gene expression profiles of metastatic neuroblastomas lacking MYCN gene amplification. J Natl Cancer Inst 2006; 98: 1193-203

31. Chang JX, Gao F, Zhao GQ, Zhang GJ. Role of NEDD9 in invasion and metastasis of lung adenocarcinoma. Exp Ther Med 2012; 4: 795-800

32. Feng Y, Wang Y, Wang Z, Fang Z, Li F, Gao Y et al. The CRTC1-NEDD9 signaling axis mediates lung cancer progression caused by LKB1 loss. Cancer Res 2012; 72: 6502-11

33. Kondo S, Iwata S, Yamada T, Inoue Y, Ichihara H, Kichikawa Y et al. Impact of the integrin signaling adaptor protein NEDD9 on prognosis and metastatic behavior of human lung cancer. Clin Cancer Res 2012; 18: 6326-38

34. Yang WH, Lan HY, Huang CH, Tai SK, Tzeng CH, Kao SY et al. RAC1 activation mediates Twist1-induced cancer cell migration. Nat Cell Biol 2012; 14: 366-74

35. Debreceni B, Gao Y, Guo F, Zhu K, Jia B, Zheng Y. Mechanisms of guanine nucleotide exchange and Rac-mediated signaling revealed by a dominant negative trio mutant. J Biol Chem 2004; 279: 3777-86

36. Mierke CT, Rosel D, Fabry B, Brabek J. Contractile forces in tumor cell migration. Eur J Cell Biol 2008; 87: 669-76

37. Fashena SJ, Einarson MB, O'Neill GM, Patriotis C, Golemis EA. Dissection of HEF1-dependent functions in motility and transcriptional regulation. J Cell Sci. 2002; 115: 99-111

FIGURE 1

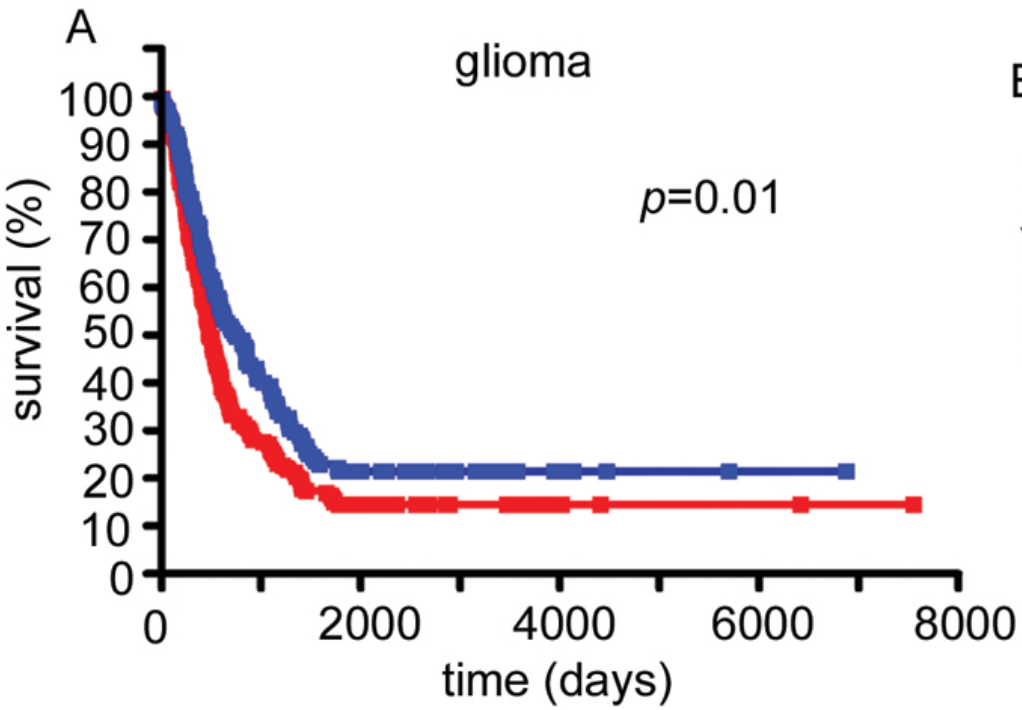
A
glioma
p=0.01
survival (%)
100
90
80
70
60
50
40
30
20
10
0
0
2000
4000
6000
8000
time (days)

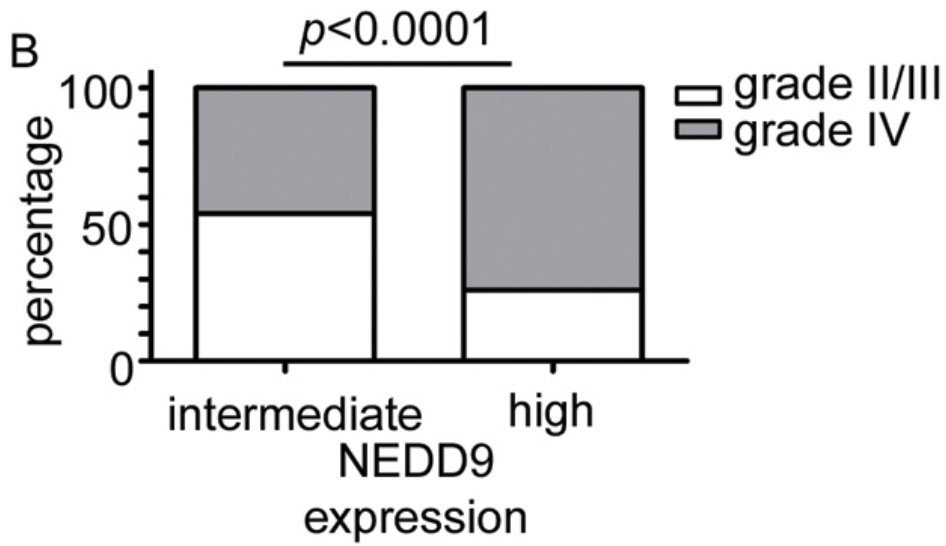
B
p<0.0001
percentage
100
50
0
grade II/III
grade IV
intermediate
high
NEDD9
expression

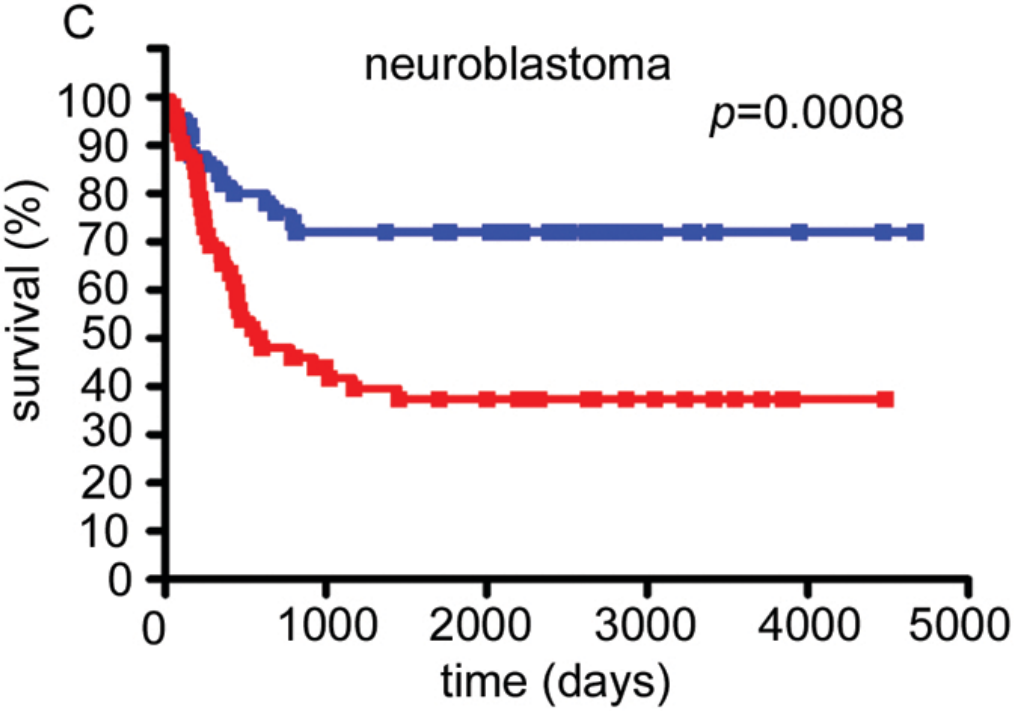
C
neuroblastoma
p=0.0008
survival (%)
100
90
80
70
60
50
40
30
20
10
0
0
1000
2000
3000
4000
5000
time (days)

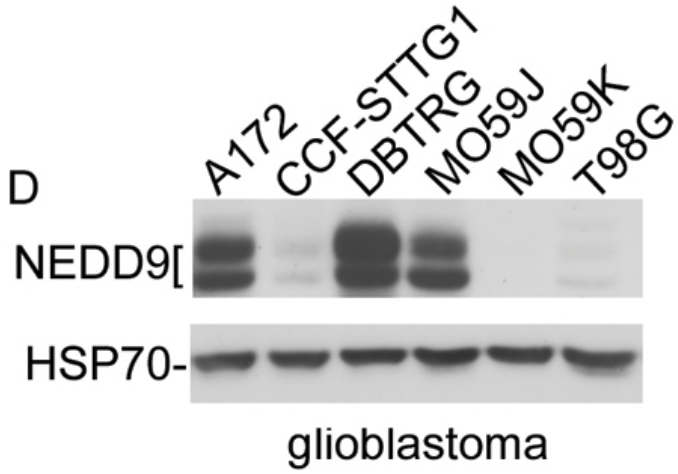
D
A172
CCF-STTG1
DBTRG
MO59J
MO59K
T98G
NEDD9[
HSP70-
glioblastoma

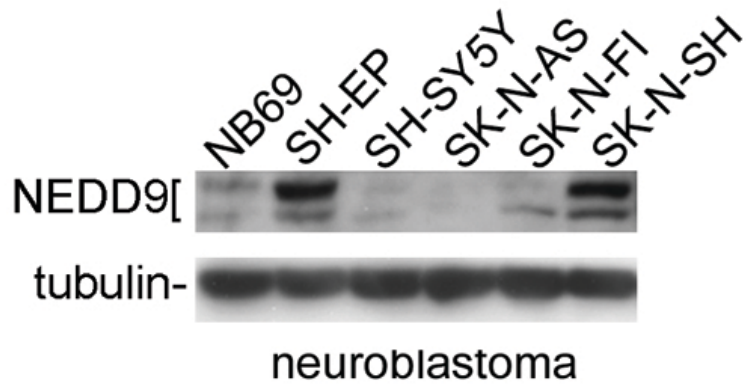
NB69
SH-EP
SH-SY5Y
SK-N-AS
SK-N-FI
SK-N-SH
NEDD9[
tubulin-
neuroblastoma

FIGURE 2

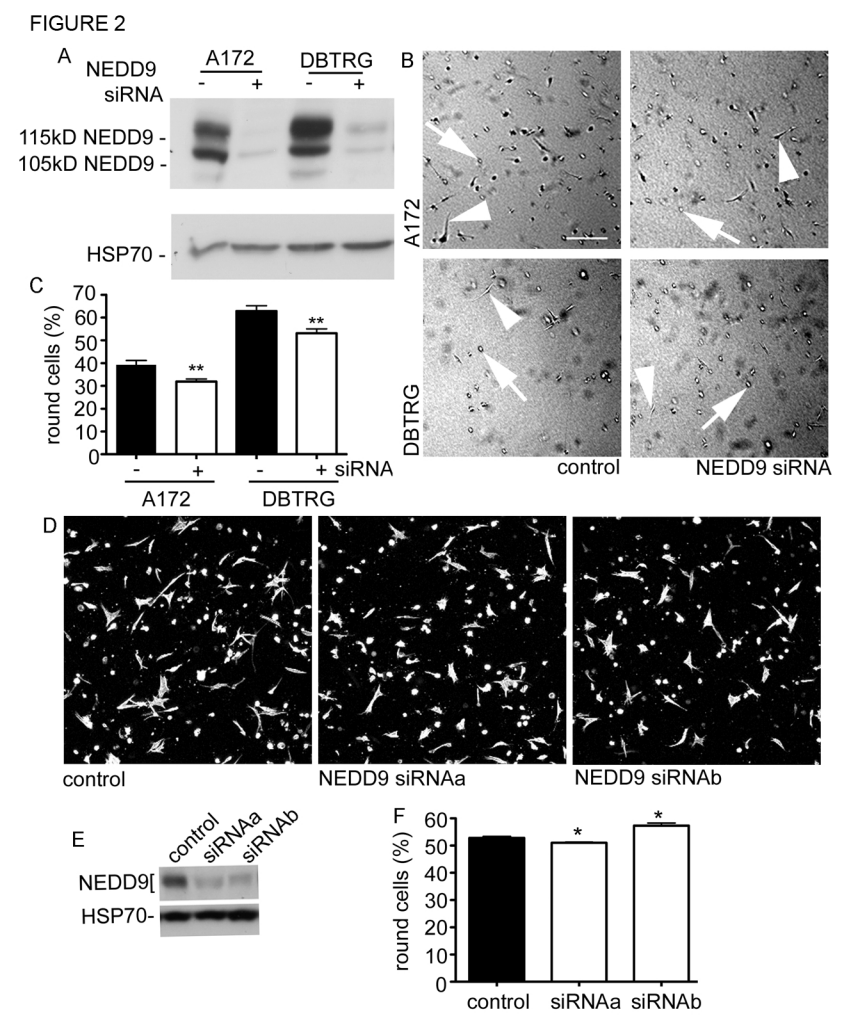
A
NEDD9
siRNA
A172
DBTRG
- + - +
115kD NEDD9 -
105kD NEDD9 -
HSP70 -
B
A172
DBTRG
control
NEDD9 siRNA
C
round cells (%)
70
60
50
40
30
20
10
0
**
**
- + - + siRNA
A172
DBTRG
D
control
NEDD9 siRNAa
NEDD9 siRNAb
E
control
siRNAa
siRNAb
NEDD9[
HSP70-
F
round cells (%)
60
50
40
30
20
10
0
*
*
control
siRNAa
siRNAb

FIGURE 3

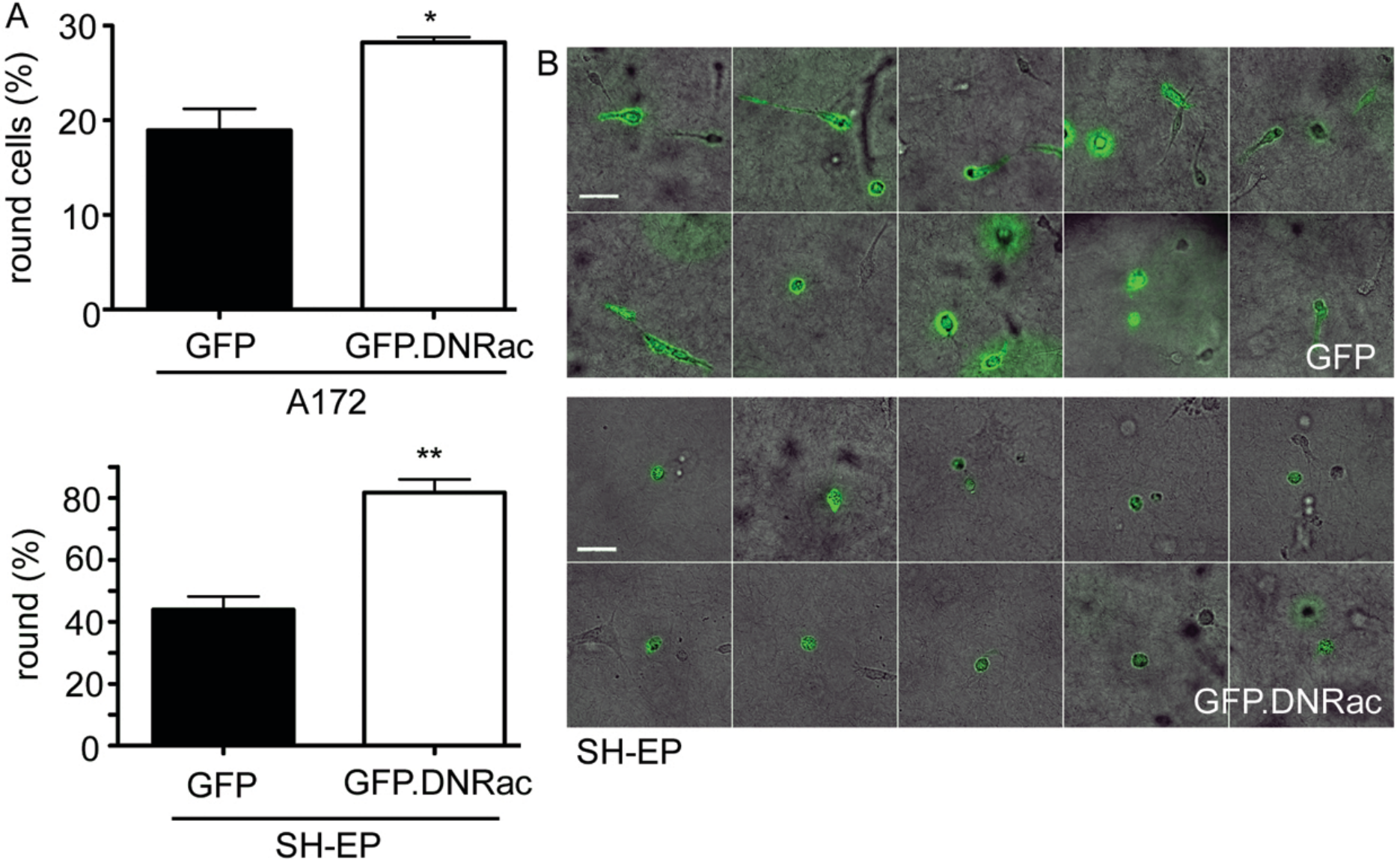
A
round cells (%)
30
20
10
0
*
GFP
GFP.DNRac
A172
round (%)
80
60
40
20
0
**
GFP
GFP.DNRac
SH-EP
B
GFP
GFP.DNRac
SH-EP

FIGURE 4

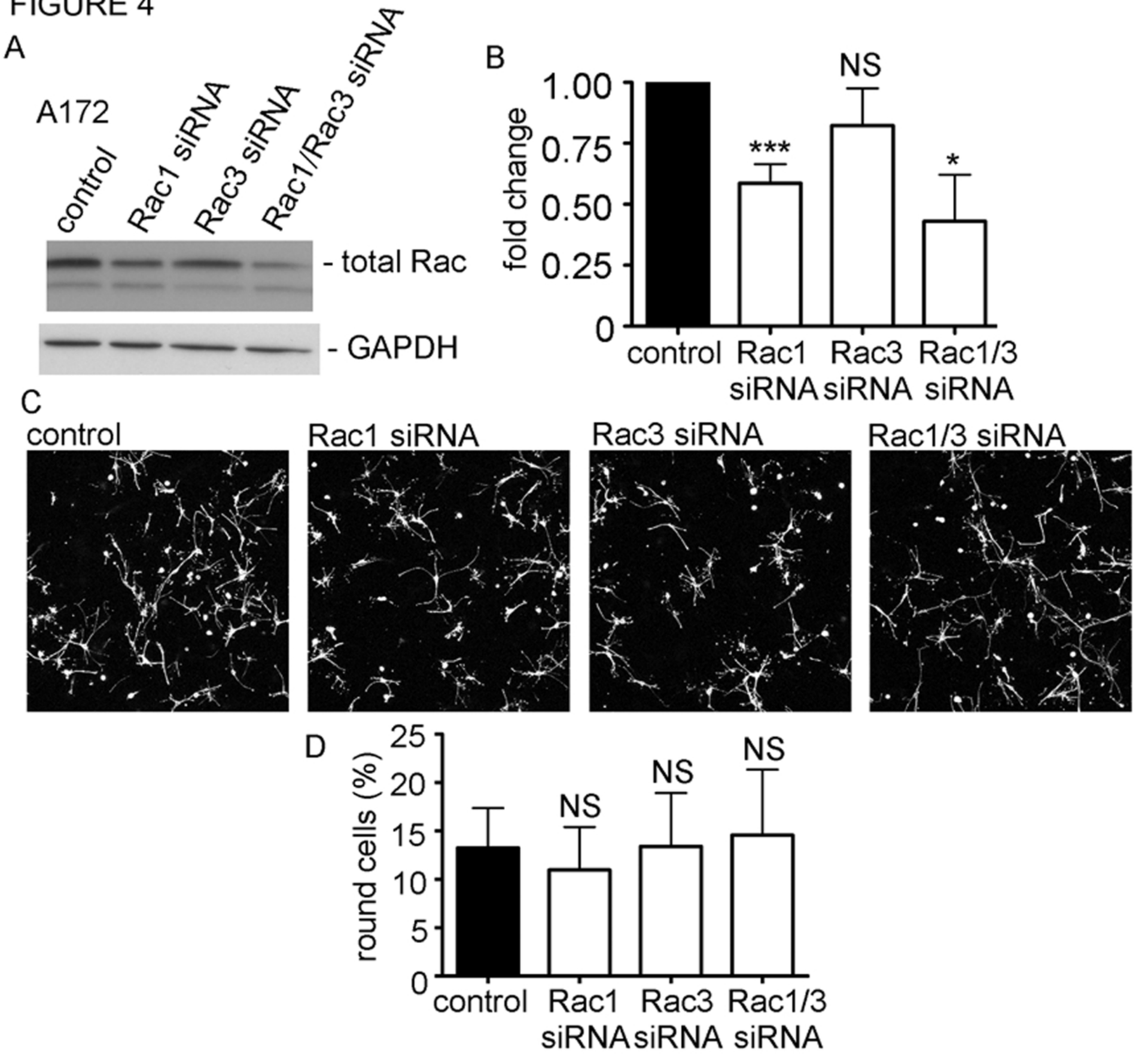
A
A172
control
Rac1 siRNA
Rac3 siRNA
Rac1/Rac3 siRNA
- total Rac
- GAPDH
B
fold change
1.00
0.75
0.50
0.25
0
***
NS
*
control
Rac1 siRNA
Rac3 siRNA
Rac1/3 siRNA
C
control
Rac1 siRNA
Rac3 siRNA
Rac1/3 siRNA
D
round cells (%)
25
20
15
10
5
0
NS
NS
NS
control
Rac1 siRNA
Rac3 siRNA
Rac1/3 siRNA

FIGURE 5

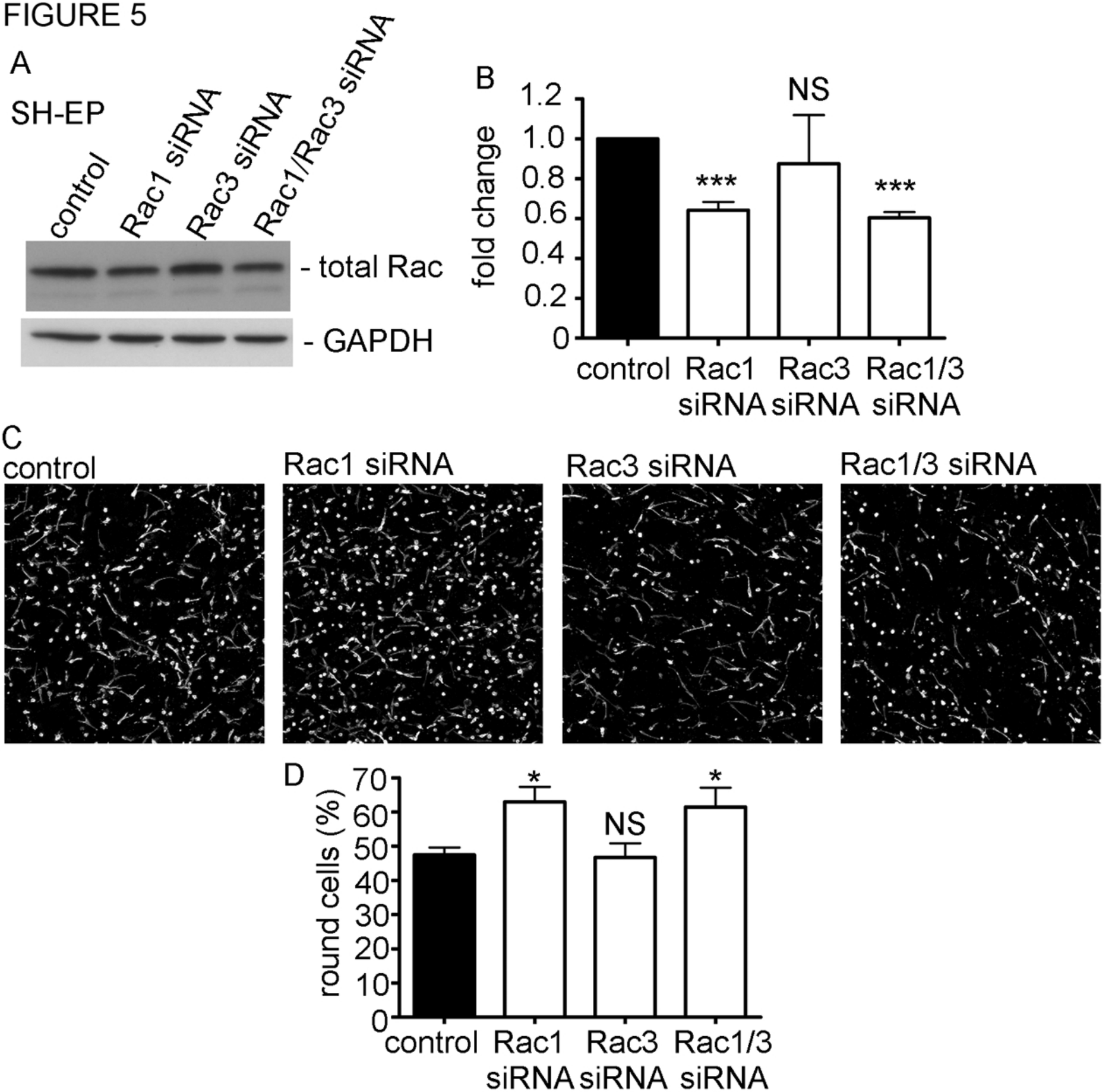
A
SH-EP
control
Rac1 siRNA
Rac3 siRNA
Rac1/Rac3 siRNA
- total Rac
- GAPDH
B
fold change
1.2
1.0
0.8
0.6
0.4
0.2
0
NS
***
***
control
Rac1 siRNA
Rac3 siRNA
Rac1/3 siRNA
C
control
Rac1 siRNA
Rac3 siRNA
Rac1/3 siRNA
D
round cells (%)
70
60
50
40
30
20
10
0
*
NS
*
control
Rac1 siRNA
Rac3 siRNA
Rac1/3 siRNA

FIGURE 6

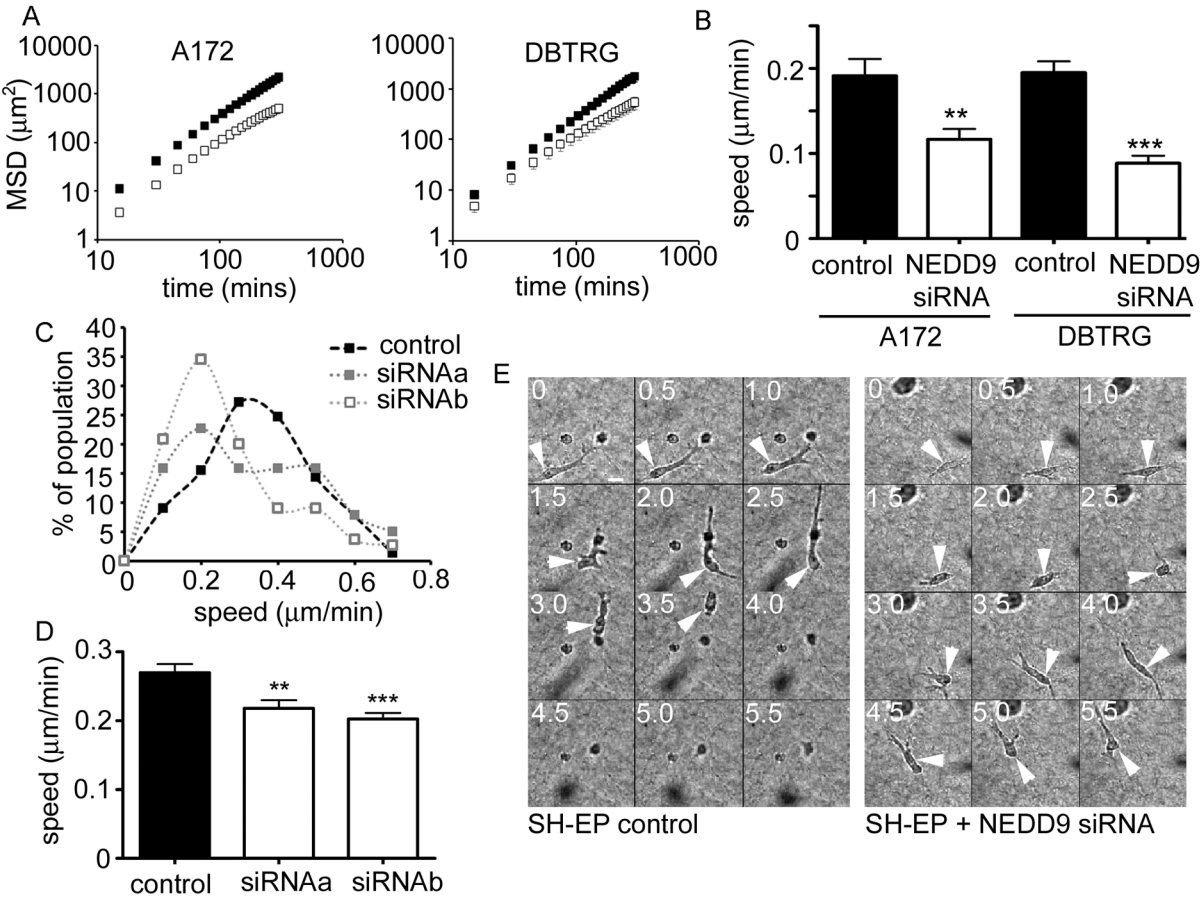
A
A172
DBTRG
MSD (μm²)
time (mins)
B
speed (μm/min)
control
NEDD9 siRNA
A172
DBTRG
C
% of population
speed (μm/min)
control
siRNAa
siRNAb
D
speed (μm/min)
control
siRNAa
siRNAb
E
SH-EP control
SH-EP + NEDD9 siRNA